Sara Grundel Lennart Jansen Nils Hornung Tanja Clees
Caren Tischendorf Peter Benner

Model Order Reduction of Differential Algebraic Equations Arising from the Simulation of Gas Transport Networks

Max Planck Institute Magdeburg
Preprints

MPIMD/13-09 **June 26, 2013**

Impressum:

Max Planck Institute for Dynamics of Complex Technical Systems, Magdeburg

Publisher:
Max Planck Institute for Dynamics of Complex Technical Systems

Address:
Max Planck Institute for Dynamics of Complex Technical Systems
Sandtorstr. 1
39106 Magdeburg

www.mpi-magdeburg.mpg.de/preprints

Max Planck Institute Magdeburg
Preprints

Sara Grundel Lennart Jansen Nils Hornung Tanja Clees
Caren Tischendorf Peter Benner

Model Order Reduction of Differential Algebraic Equations Arising from the Simulation of Gas Transport Networks

MPIMD/13-09 **June 26, 2013**

Abstract

We explore the Tractability Index of Differential Algebraic Equations (DAEs) that emerge in the simulation of gas transport networks. Depending on the complexity of the network, systems of index 1 or index 2 can arise. We then apply Model Order Reduction (MOR) techniques such as Proper Orthogonal Decomposition (POD) to a network of moderate size and complexity and show that one can reduce the system size significantly. This can be either achieved by directly reducing the original DAE formulation or by applying MOR to an index-reduced system. First numerical results are reported on.

1 Introduction

Pipeline networks for gas transport can be modelled by a directed graph $\mathscr{G} = (\mathscr{A}, \mathscr{N})$ of edges $\mathscr{A}$ and nodes $\mathscr{N}$, which defines the network topology, see [GHK$^+$13, ES]. Edges $k \in \mathscr{A}$ can e. g. represent pipes, connections, compressors, valves and regulators. Within this work we only regard a simplified network for Model Order Reduction, though, and restrict ourselves to pipe components. This simplification may be justified by several practical applications. Consider, for example, the computation of a feasable initial solution for the computation of a more complex network. This initialization can be subdivided into a series of simpler problems (i. e. simpler network components) that become increasingly more involved [GHK$^+$13]. In order to speed up the initialization procedure, it can already be helpful to reduce and thus accelerate the simpler sub-problems.

The set of nodes $\mathscr{N}$ can be partitioned into supply nodes $\mathscr{N}_+$, demand nodes $\mathscr{N}_-$ and interior nodes $\mathscr{N}_0$ (sometimes called junctions)

$$\mathscr{N} = \mathscr{N}_+ + \mathscr{N}_- + \mathscr{N}_0.$$

2 Gas transport in Pipeline Networks

We model gas transport within a single pipe segment by a simplification of the so-called isothermal Euler equations, see e. g. [GHK$^+$13, Ste07, ES, HMS10, LIW04] for more details. The isothermal Euler equations form a coupled PDE of mass and momentum balance laws together with a constitutive relation. In particular, our system of equations includes the continuity equation (1), the pressure loss equation (2) and the equation of the state of a real gas (3).

As independent variables, we consider $t \geq 0$ (time) and $x \in [0, L]$ (space), where L is the length of the segment. As dependent variables of the full isothermal equations (before simplifications), we have a density field $\rho(x,t)$, a velocity field $v(x,t)$, a pressure field $p(x,t)$ and a temperature field $T(x,t)$. We also define gas flow as $q(x,t) = \rho(x,t)\, v(x,t)$ and consider a given geodesic height $h(x)$, given diameter $D(x)$, as well as a friction coefficient $\lambda(q)$, compressibility $z(p,T)$, and the field $\gamma = RT$, where R is a gas constant.

$$\partial_t \rho + \partial_x q = 0 \tag{1}$$

$$\partial_t q + \partial_x p + \partial_x(\rho v^2) + g\rho\, \partial_x h = -\frac{\lambda(q)}{2D} \rho v |v| \tag{2}$$

$$p = \gamma(T)\, z(p,T)\, \rho \tag{3}$$

In order to simplify this system, we follow [GHK$^+$13] and approximate γz in the dependence between p and ρ (eqn.(3)) by the square of the sound velocity $a \approx 300\,\mathrm{m/s}$ of the

gas.

$$\begin{aligned} \partial_t \rho + \partial_x q &= 0 \\ \partial_t q + \partial_x p + \partial_x(\rho v^2) + g\rho\,\partial_x h &= -\frac{\lambda}{2D}\rho v|v| \\ p &= a^2\rho. \end{aligned}$$

Additionally, we replace v by q and ρ, neglect differences in geodesic height and temperature ($\forall x : h(x) \equiv h_0, T(x) \equiv T_0$) as well es kinetic energy, and yield

$$\begin{aligned} \partial_t \rho + \partial_x q &= 0 \\ \partial_t q + a^2 \partial_x \rho &= -\frac{\lambda}{2D}\frac{q|q|}{\rho}. \end{aligned} \tag{4}$$

Given the PDE for a pipe in this way, we will need to discretize it along each individual segment. Furthermore, we consider the network graph $\mathscr{G}$ and establish a mass balance equation for all interior and demand nodes as well as the boundary conditions on the gas density for the supply nodes. These mass balance equations equate to Kirchhoff's first law in electric networks. The discretization in each pipe is achieved by simple differences, while the remaining variables are replaced by simple averages. Let $d_i(t)$ be the time dependent demand at the i-th demand node and let $s_i(t)$ be the time dependent gas density at the i-th supply node. We will denote the density at node i by ρ_i and the flow of the k-th pipe at the left by q_L^k and at the right by q_R^k. In addition, we call the density at the node to the left of the k-th pipe ρ_L^k and the density at the node to the right ρ_R^k, which leads to the following set of equations

$$0 = \rho_i(t) - s_i(t) \qquad \text{for all } i \in \mathscr{N}_+ \tag{5a}$$

$$0 = \sum_{\bar{q}_R \in I_R^i} \bar{q}_R - \sum_{\bar{q}_L \in I_L^i} \bar{q}_L \qquad \text{for all } i \in \mathscr{N}_0 \tag{5b}$$

$$d_i(t) = \sum_{\bar{q}_R \in I_R^i} \bar{q}_R - \sum_{\bar{q}_L \in I_L^i} \bar{q}_L \qquad \text{for all } i \in \mathscr{N}_- \tag{5c}$$

$$\partial_t \frac{\rho_R^k + \rho_L^k}{2} = -\frac{q_R^k - q_L^k}{L_k} \qquad \text{for all } k \in \mathscr{A} \tag{5d}$$

$$\partial_t \frac{q_R^k + q_L^k}{2} = -a_k^2 \frac{\rho_R^k - \rho_L^k}{L_k} - \frac{\lambda_k}{4D_k}\frac{(q_R^k + q_L^k)|q_R^k + q_L^k|}{\rho_R^k + \rho_L^k} \qquad \text{for all } k \in \mathscr{A} \tag{5e}$$

with I_R^i the set of flows at the right of the pipes which are connected at the right to the i-th node, and I_L^i the set of flows at the left of the pipes which are connected at the left to the i-th node.

We will rewrite system (5) to obtain a matrix form of it. In order to do so, we use the incidence matrix A of the directed graph for the nodes in $\mathscr{N}_- \bigcup \mathscr{N}_0$

$$(A)_{ij} \equiv \begin{cases} 1 & \text{if edge } j \text{ leaves node } i, \\ -1 & \text{if edge } j \text{ enters node } i, \\ 0 & \text{else.} \end{cases}$$

The matrix A can be interpreted as the incidence matrix of the complete network reduced by all rows related to the supply nodes. Just like any reduced incidence matrix of a graph,

A has full row rank. The incidence matrix has a left kernel that is of dimension 1 or less. If we, however, remove at least one row, the resulting matrix A has a trivial left kernel. Notice the analogy to the electric networks. The incidence matrix of an electric network is always reduced by one reference node, which is called the mass node, see [Tis99]. The electric potential at the mass node is fixed analogously to the gas density at a supply node.

So as to set up the matrix form of (5), we also need the incidence matrix of the directed graph for the supply nodes $\mathcal{N}_+$

$$(A_S)_{ij} \equiv \begin{cases} 1 & \text{if edge } j \text{ leaves node } i, \\ -1 & \text{if edge } j \text{ enters node } i, \\ 0 & \text{else.} \end{cases}$$

These are the rows of the complete incidence matrix which where not use in A. More precisely, if you call the complete incidence matrix B, we get in Matlab notation $A_S = B(\text{supply},:)$ and $A = B(\text{nonsupply},:)$ picking either the nodes that are supplies (to form A_S) or those that are not.

Next define the incidence matrices of the undirected graph $|A|$ and $|A_S|$ as the component-wise absolute values of the incidence matrices of the directed graph. Notice that $|A|$ also has full row rank. Since the flow of a pipe on the left side must not coincide with the flow on the right side we also define two partial incidence matrices of the directed graph for the nodes $\mathcal{N}_- \bigcup \mathcal{N}_0$

$$(A_L)_{ij} \equiv \begin{cases} -1 & \text{if edge } j \text{ enters node } i, \\ 0 & \text{else.} \end{cases}$$

and

$$(A_R)_{ij} \equiv \begin{cases} 1 & \text{if edge } j \text{ leaves node } i, \\ 0 & \text{else.} \end{cases}.$$

These partial incidence matrices are tightly linked to the matrix A

$$A = A_R + A_L \text{ and } |A| = A_R - A_L.$$

In addition to the previous definitions, let $\rho = \begin{pmatrix} \rho_s & \rho_d \end{pmatrix}$ with ρ_s the density at the supply nodes and ρ_d the density at the demand nodes and junctions. Moreover, define two material-dependent matrices $M_L = \text{diag}(\ldots \frac{L_k}{4} \ldots)$ and $M_a = \text{diag}(\ldots - \frac{a_k^2}{L_k} \ldots)$, as well as a function g, component-wise for every pipe, by

$$g_k\left(\frac{q_R^k + q_L^k}{2}, \rho_R^k, \rho_L^k\right) = -\frac{\lambda_k}{D_k} \frac{\frac{q_R^k+q_L^k}{2}\left|\frac{q_R^k+q_L^k}{2}\right|}{\rho_R^k + \rho_L^k}.$$

By defining the vector of all right flows of all pipes $q_R = \begin{pmatrix} \ldots & q_R^k & \ldots \end{pmatrix}$ and all left flows of all pipes $q_L = \begin{pmatrix} \ldots & q_L^k & \ldots \end{pmatrix}$ as well as the vector of demands $d(t) = \begin{pmatrix} \ldots & d_i(t) & \ldots \end{pmatrix}$ where for nodes in $\mathcal{N}_0$ the demands are 0 we are finally able to denote (5) in matrix form.

$$0 = \rho_s - s(t) \tag{6a}$$
$$0 = A_R q_R + A_L q_L - d(t) \tag{6b}$$
$$|A_S|^T \partial_t \rho_s + |A|^T \partial_t \rho_d = -M_L^{-1} \frac{q_R - q_L}{2} \tag{6c}$$
$$\partial_t \frac{q_R + q_L}{2} = M_a (A_S^T \rho_s + A^T \rho_d) + g\left(\frac{q_R + q_L}{2}, \rho_s, \rho_d\right) \tag{6d}$$

One can write in short form

$$E\dot{x} = Hx + f(x,t) \tag{7}$$

where $x = \begin{pmatrix} \rho_s & \rho_d & q_R & q_L \end{pmatrix}^T$, $f(x,t) = \begin{pmatrix} -s(t) & -d(t) & 0 & g\left(\frac{q_R+q_L}{2}, \rho_s, \rho_d\right) \end{pmatrix}^T$ and the matrices are given by

$$E = \begin{pmatrix} 0 & 0 & 0 & 0 \\ 0 & 0 & 0 & 0 \\ |A_S^T| & |A^T| & 0 & 0 \\ 0 & 0 & \frac{1}{2}I & \frac{1}{2}I \end{pmatrix}, \quad H = \begin{pmatrix} I & 0 & 0 & 0 \\ 0 & 0 & A_R & A_L \\ 0 & 0 & -\frac{1}{2}M_L^{-1} & \frac{1}{2}M_L^{-1} \\ M_a A_S & M_a A & 0 & 0 \end{pmatrix}.$$

The parameters in the system are λ_k, a_k, L_k, D_k. These parameters are known at least within some range of uncertainty. It is crucial to make sure that the reduced model can handle small variations of those parameters. The functions $s(t)$ and $d(t)$ are considered as input functions. They are time dependent but within a certain class of functions. One is interested in reduced-order models which give good results for a large class of such input functions.

3 Tractability Index

There are several different concepts for the index. For a survey refer to [Meh13]. We will use the Tractability Index due to Maerz [LMT13]. In particular, we will apply the concept of the Tractability Index to an equation given in the form (7). This equation is an Ordinary Differential Equation if E has full rank. In the following, we introduce the matrices G_0, G_1, G_2 such that either G_1 does not have full rank and the system has index 2 if G_2 has full rank, or the system has index 1 if G_1 already has full rank. The sequence is given by

$$G_0 = E \tag{8a}$$
$$G_1 = G_0 + B_0 Q_0 \tag{8b}$$
$$G_2 = G_1 + B_1 Q_1. \tag{8c}$$

Here the Q_i are projectors onto the kernel of G_i. Therefore, we see immediately that $Q_1 = 0$ and $G_2 = G_1$ if G_1 has full rank. Furthermore, $B_0 = H + J_x f$ and $B_1 = B_0 P_0$ where $P_0 = 1 - Q_0$. This series will in theory also give a recipe on how to compute projection matrices to decouple the algebraic from the differential part. This is, however, computationally expensive. In the next section we will see that in the case of the gas network equations we can reduce the equations to an ODE without computing the projector matrices explicitly. The resulting ODE is easy to simulate and reduce.

4 Index Analysis and Reduction

In this section the Tractability Index of the DAE (6) will be analyzed. Furthermore, a reduction procedure will be presented such that (6) can be reduced to an ordinary differential equation in descriptor form.

For the index analysis we use the invariance of the Tractability Index with respect to constant transformations and refactorizations, see [LMT13]. We prove that the Tractability Index of (6) is equal or lower than two in two steps. In the first step, we prove that a certain DAE prototype is always of index 2 or lower, and secondly, we convert (6) into a DAE of the prototype form (9) by constant transformations and refactorizations only. Consider the following class of DAEs

$$\partial_t x_1 = f(x_1, x_2, y_1, y_2, t) \tag{9a}$$
$$0 = x_2 - s(t) \tag{9b}$$
$$0 = y_1 + g(x_1, x_2, y_2, t) \tag{9c}$$
$$M\partial_t x_2 = y_2 \tag{9d}$$

with the partial derivatives $f_{x_1}, f_{x_2}, f_{y_1}$ and f_{y_2} of f and the partial derivatives g_{x_1}, g_{x_2} and g_{y_2} of g.

Lemma 4.1 *Equations of type* (9) *are always of Tractability Index 2 or lower.*

Proof The first sequence of the matrix chain of the Tractability Index is given by

$$G_0 = \begin{pmatrix} I & 0 & 0 & 0 \\ 0 & 0 & 0 & 0 \\ 0 & 0 & 0 & 0 \\ 0 & M & 0 & 0 \end{pmatrix}, \; Q_0 = \begin{pmatrix} 0 & 0 & 0 & 0 \\ 0 & Q & 0 & 0 \\ 0 & 0 & I & 0 \\ 0 & 0 & 0 & I \end{pmatrix}, \; P_0 = \begin{pmatrix} I & 0 & 0 & 0 \\ 0 & P & 0 & 0 \\ 0 & 0 & 0 & 0 \\ 0 & 0 & 0 & 0 \end{pmatrix}, \; B_0 = \begin{pmatrix} f_{x_1} & f_{x_2} & f_{y_1} & f_{y_2} \\ 0 & I & 0 & 0 \\ g_{x_1} & g_{x_2} & I & g_{y_2} \\ 0 & 0 & 0 & I \end{pmatrix}$$

with Q a projector onto $\ker M$ and $P = I - Q$ the complementary projector. Clearly we have then that $PQ = QP = MQ = 0$ and $MP = M$. Hence we obtain

$$G_1 = G_0 + B_0 Q_0 = \begin{pmatrix} I & f_{x_2} Q & f_{y_1} & f_{y_2} \\ 0 & Q & 0 & 0 \\ 0 & g_{x_2} Q & I & g_{y_2} \\ 0 & M & 0 & I \end{pmatrix}, \; B_1 = B_0 P_0 = \begin{pmatrix} f_{x_1} & f_{x_2} P & 0 & 0 \\ 0 & P & 0 & 0 \\ g_{x_1} & g_{x_2} P & 0 & 0 \\ 0 & 0 & 0 & 0 \end{pmatrix}.$$

At this point we already see that the DAE (9) has index 1 if and only if $M = 0$ or (9d) vanishes completely. Otherwise we calculate

$$Q_1 = \begin{pmatrix} 0 & K & 0 & 0 \\ 0 & P & 0 & 0 \\ 0 & g_{y_2} M & 0 & 0 \\ 0 & -M & 0 & 0 \end{pmatrix}, \; G_2 = G_1 + B_1 Q_1 = \begin{pmatrix} I & f_{x_1} K + f_{x_2} & f_{y_1} & f_{y_2} \\ 0 & I & 0 & 0 \\ 0 & g_{x_1} K + g_{x_2} & I & g_{y_2} \\ 0 & M & 0 & I \end{pmatrix}.$$

with $K \equiv (f_{y_2} - f_{y_1} g_{y_2}) M$. Notice that G_2 is always non-singular, hence the DAE is of index 2 or lower.

Finally, we need to show that (6) can be converted into (9) under constant transformations and refactorizations.

Lemma 4.2 *(i) System* (6) *has Tractability Index 2 or lower. (ii) More precisely, there exists a conversion of* (6) *by index-invariant transformations to the system*

$$\begin{aligned}
\partial_t \rho_m &= -(V_1^T |A^T|)^{-1} q_1 \\
\partial_t q_+ &= \tilde{g}(q_+, \rho_s, \rho_m) \\
0 &= \rho_s - s(t) \\
0 &= q_1 - (|A| M_L V_1)^{-1} (d(t) - A q_+ - |A| M_L W_1 V_2 q_2) \\
0 &= q_3 \\
-V_2^T W_1^T |A_S^T| \partial_t \rho_s &= q_2
\end{aligned} \tag{10}$$

for variables $\rho_m, q_1, q_2, q_3, q_+$ *and projection matrices* V_1, V_2, W_1. *This system, with* $M = -V_2^T W_1^T |A_S^T|$ *and*

$$x_1 = \begin{pmatrix} \rho_m \\ q_+ \end{pmatrix}, \quad x_2 = (\rho_s), \quad y_1 = \begin{pmatrix} q_1 \\ q_3 \end{pmatrix}, \quad y_2 = (q_2),$$

is then in the form of (9).

Proof Clearly, *(i)* follows from *(ii)*, so that it suffices to show the latter. First define

$$q_+ \equiv \frac{q_R + q_L}{2} \text{ and } q_- \equiv \frac{q_R - q_L}{2},$$

which leads to a constant transformation

$$\begin{pmatrix} q_R \\ q_L \end{pmatrix} = \begin{pmatrix} I & I \\ I & -I \end{pmatrix} \begin{pmatrix} q_+ \\ q_- \end{pmatrix}$$

such that (6) can be written as

$$\begin{aligned}
|A_S^T| \partial_t \rho_s + |A^T| \partial_t \rho_d &= -M_L^{-1} q_- \\
\partial_t q_+ &= M_a (A_S^T \rho_s + A^T \rho_d) + g(q_+, \rho_s, \rho_d) \\
0 &= A q_+ + |A| q_- - d(t) \\
0 &= \rho_s - s(t).
\end{aligned} \tag{11}$$

Next define four orthonormal bases. Let V_1 be an orthonormal basis of $\operatorname{coker}|A| = \operatorname{im}(|A|^T)$ and let W_1 be an orthonormal basis of $\ker|A|$. Then W_1 and V_1 span the whole edge space. Let V_2 be an orthonormal basis of $\operatorname{coker}|A_S|W_1$ and let W_2 be an orthonormal basis of $\ker|A_S|W_1$. These bases could be related to the topology of the network but for our purposes this is not necessary. Notice that

$$\begin{pmatrix} V_1^T \\ V_2^T W_1^T \\ W_2^T W_1^T \end{pmatrix} = \begin{pmatrix} I & 0 \\ 0 & V_2^T \\ 0 & W_2^T \end{pmatrix} \begin{pmatrix} V_1^T \\ W_1^T \end{pmatrix} \tag{12}$$

is a constant non-singular matrix due to the definition of the orthonormal bases. Since kernel and cokernel partition the edge space into two complementary subspaces, (12)

constitutes an iterated partitioning procedure. Notice also that we have $|A|W_1 = 0$ and $|A_S|W_1W_2 = 0$. Hence we obtain

$$\begin{aligned}
V_1^T|A_S^T|\partial_t\rho_s + V_1^T|A^T|\partial_t\rho_d &= -V_1^T M_L^{-1} q_- \\
V_2^T W_1^T|A_S^T|\partial_t\rho_s &= -V_2^T W_1^T M_L^{-1} q_- \\
\partial_t q_+ &= M_a(A_S^T\rho_s + A^T\rho_d) + g(q_+,\rho_s,\rho_d) \\
0 &= -W_2^T W_1^T M_L^{-1} q_- \\
0 &= Aq_+ + |A|q_- - d(t) \\
0 &= \rho_s - s(t)
\end{aligned}$$

by a constant refactorization, which means we multiplied the first equation of (11) from the left by (12). After this refactorization we also use the bases for a constant transformation

$$q_- = M_L(W_1W_2q_3 + W_1V_2q_2 + V_1q_1),$$

which leads to

$$\begin{aligned}
V_1^T|A^T|\partial_t((V_1^T|A^T|)^{-1}V_1^T|A_S^T|\rho_s + \rho_d) &= -q_1 \\
V_2^T W_1^T|A_S^T|\partial_t\rho_s &= -q_2 \\
\partial_t q_+ &= M_a(A_S^T\rho_s + A^T\rho_d) + g(q_+,\rho_s,\rho_d) \\
0 &= -q_3 \\
0 &= Aq_+ + |A|M_LV_1q_1 + |A|M_LW_1V_2q_2 \\
&\quad + |A|M_LW_1W_2q_3 - d(t) \\
0 &= \rho_s - s(t).
\end{aligned}$$

The eventual transformation is defined by

$$\rho_m = (V_1^T|A^T|)^{-1}V_1^T|A_S^T|\rho_s + \rho_d$$

which leads to the desired equations if

$$\begin{aligned}
\tilde{g}(q_+,\rho_s,\rho_m) =& M_a(A_S^T\rho_S + A^T(\rho_m - (V_1^T|A^T|)^{-1}V_1^T|A_S^T|\rho_s) \\
&+ g(q_+,\rho_S,\rho_m - (V_1^T|A^T|)^{-1}V_1^T|A_S^T|\rho_s).
\end{aligned}$$

We obtain

$$\partial_t\rho_m = -(V_1^T|A^T|)^{-1}q_1 \tag{13a}$$
$$\partial_t q_+ = \tilde{g}(q_+,\rho_s,\rho_m) \tag{13b}$$
$$0 = \rho_s - s(t) \tag{13c}$$
$$0 = q_1 - (|A|M_LV_1)^{-1}(d(t) - Aq_+ - |A|M_LW_1V_2q_2) \tag{13d}$$
$$0 = q_3 \tag{13e}$$
$$-V_2^T W_1^T|A_S^T|\partial_t\rho_s = q_2. \tag{13f}$$

Notice that we can eliminate q_3 in (13a) and (13d) as a constant refactorization. With $M = -V_2^T W_1^T|A_S^T|$ and

$$x_1 = \begin{pmatrix}\rho_m \\ q_+\end{pmatrix}, \quad x_2 = \begin{pmatrix}\rho_s\end{pmatrix}, \quad y_1 = \begin{pmatrix}q_1 \\ q_3\end{pmatrix}, \quad y_2 = \begin{pmatrix}q_2\end{pmatrix}$$

system (13) has the structure of the DAE class (9). Hence it has index 1 if $V_2^T W_1^T |A_S^T| = 0$ or (13f) vanishes completely, else it has index 2.

Remark: This condition for index 1 can be expressed by the topological condition that there is only one supply node in the system. To prove that the used orthonormal matrices would have to be chosen with a topological meaning. One can then show that if the gas network has only one supply node it is always index 1 and if it has more it has to be index 2. We will not prove this in detail here as it is not of practical interest since most realistic examples with have more than 1 supply node and be of index 2 therefore.

For practical reasons system (13) is not necessarily well-suited, since the calculation of V_1, W_1, V_2, W_2 might increase the overall numerical error, and additionally, we do not want to invert $V_1^T |A^T|$ if the network is large.

Therefore, step back to (11)

$$|A_S^T| \partial_t \rho_s + |A^T| \partial_t \rho_d = -M_L^{-1} q_- \tag{14a}$$
$$\partial_t q_+ = M_a (A_S^T \rho_s + A^T \rho_d) + g(q_+, \rho_s, \rho_d) \tag{14b}$$
$$0 = A q_+ + |A| q_- - d(t) \tag{14c}$$
$$0 = \rho_s - s(t) \tag{14d}$$

and remember that M_L^{-1} is a diagonal matrix, hence it is very cheap to invert. Multiply (14a) from the left by $|A| M_L$ and replace $|A| q_-$ and ρ_s with the help of the (14c) and (14d) afterwards.

$$|A_S^T| \partial_t \rho_s + |A^T| \partial_t \rho_d = -M_L^{-1} q_- \tag{15a}$$
$$\Rightarrow |A| M_L |A_S^T| \partial_t \rho_s + |A| M_L |A^T| \partial_t \rho_d = -|A| q_- \tag{15b}$$
$$\Rightarrow |A| M_L |A^T| \partial_t \rho_d = A q_+ - d(t) - |A| M_L |A_S^T| \partial_t s(t) \tag{15c}$$

We need the derivative of the supply input functions to obtain (15c). Hence this step includes an index reduction. Since we only differentiate an input function, no complications like the drift-off phenomena are expected. We also replace ρ_s in (14b) with the help of (14d) and obtain a system in ρ_d and q_+.

$$|A| M_L |A^T| \partial_t \rho_d = A q_+ - d(t) - |A| M_L |A_S^T| \partial_t s(t) \tag{16a}$$
$$\partial_t q_+ = M_a A^T \rho_d + g(q_+, s(t), \rho_d) + L_a A_S^T s(t) \tag{16b}$$

$|A| M_L |A^T|$ is positive definite and symmetric since $|A^T|$ has full column rank and M_L is a positive definite diagonal matrix, hence (16) is an implicit ODE of the form

$$\begin{aligned} M \partial_t x_1 &= A x_2 + f_1(t) \\ \partial_t x_2 &= f_2(x_1, x_2, t) \end{aligned} \tag{17}$$

with M being symmetric and positive definite. This allows for a straightforward application of half-implicit solvers and MOR methods. After we have calculated ρ_d and q_+ by solving the ODE, the rest of the variables can be computed in a post processing step.

A similar decoupling result for water transport networks can be found in [JP13]. The general concept of this decoupling strategy is described in greater detail in [Jan13]. The concept arises as a mix of the Tractability Index and the Strangeness Index.

5 Model Order Reduction – POD

The gas transport equations we are considering are given in the form of (7) and thus capture (17)

$$E(p)\dot{x} = H(p)x + f(x,p,u).$$

Given such an equation our goal is reduction by projection. This means we want to find a linear subspace in which the solution trajectory lies approximately. This subspace is defined by a projection matrix $W \in \mathbb{R}^{n\times\hat{n}}$ where hopefully $\hat{n} \ll n$. More precisely, we are interested in finding a solution $\hat{x}(t) \in \mathbb{R}^{\hat{n}}$ such that

$$x(t) \approx W\hat{x}.$$

We can then reduce the given equation onto that subspace by a Galerkin projection resulting in the reduced equation

$$W^T E(p)W\dot{\hat{x}} = W^T H(p)W\hat{x} + W^T f(W\hat{x},p,u).$$

If E is a positive definite matrix then the reduced order matrix $\hat{E} = W^T EW$ will also be a positive definite matrix. If E is indefinite, possibly singular, problems are manifold. For example, a nonsingular E does not necessarily result in a nonsingular $\hat{E}$, which in general means that projection can lead to a DAE of higher index than the original one. In order to create a reduced order model, i. e. to find the subspace or compute W, we have to pick a Model Order Reduction technique. We will employ a method that is very common for nonlinear problems, the so called Proper Orthogonal Decomposition (POD). It is relatively straightforward conceptually. POD is, however, mostly used for Ordinary Differential Equations (ODEs), while we use it on the original DAE equations, too, for comparison. Some related work for linear problems can be found in [RR11] In the following, POD is introduced for the ODE case. Section 5.2 will exactly explain how we use POD in order to create our reduced order model.

5.1 Proper Orthogonal Decomposition

We will explain the basic idea of POD-MOR first. This method is also referred to as the method of snapshots [Sir87]. As explained above we are interested in finding a matrix W such that the solution trajectory is well approximated. If we assume that W has orthonormal columns $u_1,\dots,u_r$ we are interested in solving the following optimization problem

$$\min \int_0^T \left\| x(t) - \sum \langle x(t), u_i\rangle u_i \right\|^2 \mathrm{d}t \quad \text{where} \quad \langle u_i, u_j\rangle = \delta_{ij}. \tag{18}$$

The norm can be any norm, in general, but should be connected to an inner product. Since this problem is in general not solvable we take snapshots at several time steps $t_0\dots,t_N$ and find the best approximating linear subspace by solving the following problem instead

$$\min_{u_1,\dots,u_\ell} \sum_{k=1}^{N} w_k \left\| x_k - \sum_{i=1}^{\ell} \langle x_k, u_i\rangle u_i \right\|^2 \quad \text{where} \quad \langle u_i, u_j\rangle = \delta_{ij}. \tag{19}$$

For $w_i = 1$ and the inner product and norm being the standard Euclidean one, the solution to this problem is directly connected to the singular value decomposition of the matrix $Y = [x_1,\dots,x_N]$. Given the SVD of $Y = U\Sigma V^T$ the solution to (19) for the standard Euclidean inner product and Euclidean norm is obtained by the first ℓ left singular vectors which are

the first ℓ columns of U. Here we assume that the singular values in Σ are ordered. Per definition of the SVD U and V are orthogonal matrices and Σ is a diagonal matrix.

Let u_i be the singular vectors of the snapshot matrix $Y = [x(t_1), \dots, x(t_N)]$ as in [GHK+13]. Then for all time steps t_k

$$x(t_k) \approx \sum_{i=1}^{\ell} \langle x(t_k), u_i \rangle u_i = \sum_{i=1}^{\ell} \hat{x}_i(t_k) u_i = W \hat{x}(t_k)$$

where $W = [u_1, \dots, u_N]$. Though this relation does not yield for arbitrary time steps, we assume certain continuity properties of $x(t)$ and as a result

$$x(t) \approx W \hat{x}(t).$$

If we have weights w_i and the inner product is given by a weighted inner product

$$\langle x, y \rangle_E = x^T E y$$

for a symmetric positive definite matrix E we can still solve

$$\min_{u_1,\dots,u_\ell} \sum_{k=1}^{N} w_k \left\| x_k - \sum_{i=1}^{\ell} \langle x_k, u_i \rangle_E u_i \right\|_E^2 \quad \text{where} \quad \langle u_i, u_j \rangle_E = \delta_{ij}. \tag{20}$$

by a singular value decomposition. The following lemma is a known result see for example [KV02].

Lemma 5.1 *The solution to* (20) *is given by*

$$u_i = Y D^{1/2} \phi_i / \sigma_i$$

where ϕ_i are the singular vectors and σ_i^2 the singular values of $\hat{Y}^T \hat{Y} = D^{1/2} Y^T E Y D^{1/2}$

Proof

$$\begin{aligned} & \min_{u_1,\dots,u_\ell} \sum_{k=1}^{N} w_k \left\| x_k - \sum_{i=1}^{\ell} \langle x_k, u_i \rangle_E u_i \right\|_E^2 \\ \Leftrightarrow & \min_{u_1,\dots,u_\ell} \sum_{k=1}^{N} \left\| \sqrt{w_k} x_k - \sum_{i=1}^{\ell} \langle \sqrt{w_k} x_k, u_i \rangle_E u_i \right\|_E^2 \\ \Leftrightarrow & \min_{u_1,\dots,u_\ell} \sum_{k=1}^{N} \left\| \sqrt{w_k} E^{1/2} x_k - \sum_{i=1}^{\ell} \langle E^{1/2} \sqrt{w_k} x_k, E^{1/2} u_i \rangle E^{1/2} u_i \right\|^2 \end{aligned}$$

As a result, the problem is equivalent to the above and the solution is given by finding the singular value decomposition of $\hat{Y} = E^{1/2} Y D^{1/2}$ and then multiplying the resulting vectors by $E^{-1/2}$. This could possibly be too expensive as we have to find the square root of E and its inverse. Notice, however, that the vectors we are interested in are given by $E^{-1/2} U$. Thus let us instead look at the SVD of $\hat{Y} = E^{1/2} Y D^{1/2} = U \Sigma V^T$ which leads to

$$E^{-1/2} U = Y D^{1/2} V \Sigma^{-1}.$$

Here Σ and V can be computed by the SVD of $\hat{Y}^T \hat{Y} = D^{1/2} Y^T E Y D^{1/2}$. Consequently, we can compute the basis functions without computing matrix functions of E.

Given an ODE in descriptor form with a symmetric positive definite E matrix, we typically use this very E matrix as the inner product weight. In case of a DAE it is not obvious what inner weight one should use and whether the standard Euclidean inner product should, for example, be employed to create a reduced order model. Neither is it obvious whether the reduction might raise the index of the equations if one compares the reduced system to the original one. This should, in general, be avoided. For a careful application of these concepts with reportedly good results we refer to the literature [HK12].

5.2 POD for Gas Transport Simulation

The solution of the gas transport equations gives different time series for different values of the parameters and the input functions. One would be interested in a reduced order model which gives good results for all or, more realistically, for a large class of input functions and a certain parameter range. In order to achieve that, we need to solve the full system for several parameters and input functions. Based on the obtained solution data one can then create a reduced-order model. Most of the numerical tests show that these equations are intrinsically significantly reducable. Actual Parametric Model Order Reduction techniques, which consider what happens for different parameter values, have not been applied, however. We mostly assume that we know the parameters and that they are given.

In the case of the ODE (17) we could use standard POD techniques with the inner product matrix E and weights depending on the times series given. For equal time steps one would typically also want all weights to be the same, otherwise they are adjusted accordingly, which depends on the chosen quadrature rule. We assume equal time steps in this work, though. It turns out, however, that if we compute W directly from there and project our equations, the resulting reduced order model is very difficult to simulate. We therefore use POD for the time series of the pressures and for the time series of the average fluxes independently as it was also done in [HK12]. First we create projection matrices W_p and W_q leading to an overall projection matrix

$$W = \begin{bmatrix} W_p & 0 \\ 0 & W_q \end{bmatrix}.$$

In the numerical examples shown in Sect. 6 for the original DAE, we just employ standard POD on the given snapshot together with the Euclidean norm.

Remark: We believe that one can get better results if the components are projected independently but this approach has neither been tested nor explored conceptually here. Projecting them independently will probably result in a DAE whose index is not higher than the index of the original one.

6 Numerical Examples

The numerical example we study in most detail is a very simple one from [GHK$^+$13] and since it has just one supply node it actually just has Tractability Index 1. Even there, however, a lot of the difficulties in constructing a reduced order model can be experienced. These difficulties might become crucial for larger systems. We will therefore give numerical evidence that, for this simple example and a more involved one, the presented index reduction technique results in an ODE that can be stably solved, even when the original system experiences complications. In the following, we also give numerical results

segment	$L_{1,2}$	$L_{2,3}$	$L_{3,4}$	$L_{4,5}$	$L_{5,6}$	$L_{5,7}$	$L_{7,8}$	$L_{7,9}$
length	46 m	7 m	3080 m	4318 m	323 m	790 m	1820 m	1460 m
segment	$L_{9,10}$	$L_{10,11}$	$L_{11,12}$	$L_{11,13}$	$L_{13,14}$	$L_{13,15}$	$L_{15,17}$	$L_{15,16}$
length	2368 m	1410 m	296 m	3979 m	119 m	3881 m	687 m	6114 m

Table 1: Pipe lengths of the simple network, numbering in accordance with Fig. 1

node	d_4	d_8	d_9	d_{10}	d_{12}	d_{14}	d_{16}	d_{17}
demand	0.21 kg/s	34.86 kg/s	0.22 kg/s	2.83 kg/s	1.81 kg/s	1.04 kg/s	2.85 kg/s	1.45 kg/s

Table 2: Fluxes at the demand nodes of the simple network, numbering in accordance with Fig. 1

on Model Order Reduction applied to the index-reduced ODE. As expected, the results are promising and indicate that the presented combinations of approaches may be stably applicable in practice.

For a detailed description of the first example, see [GHK+13] and Fig. 1. Its topology consists of 17 nodes, among which there are 8 demand nodes and a single supply, simply connected by a net of 16 pipes. The lengths of the individual pipes are given as shown in Table 1, while the pipe diameter and friction coefficients remain constant throughout the entire network ($D = 0.206\,\mathrm{m}$, $\lambda = 0.0003328$). The supply at time $t_0 = 0$ is given by $S_0 = 44.5\,\mathrm{bar}$, the demands vary from node to node, see Table 2. We assume a single gas phase specified by $a_k = 430.5\,\mathrm{m/s}$ for all k.

As to the simple network we report on two different scenarios or settings. In both scenarios, we fix the demands in time and lower the supply pressure within a given time interval. Such a situation arises in practice if variations in the supply are to be investigated. A change in the input functions may also be relevant in the problem of finding a feasible starting solution. For our test the supply pressure function in time is given by

$$s(t) = (1 - 0.1(\cos(t\pi/1000) - 1))\, S_0,$$

$t \in [0, 20000]$ in seconds, which resembles – except for a small numerical error – the

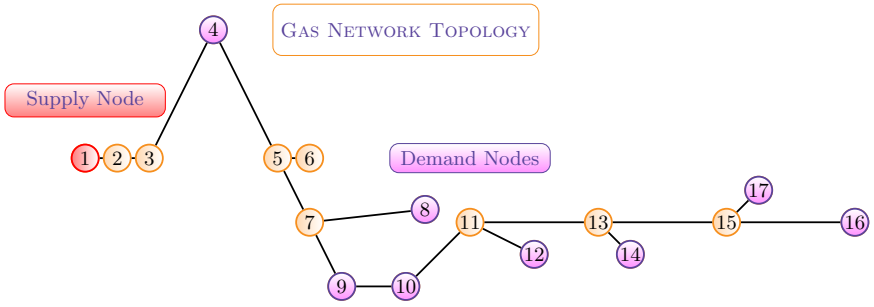

Figure 1: Gas network graph

reduction order	2	4	6	8	10	12	14	16	18	20
scenario 1	1.06	1.6	0.016	0.012	0.01	0.01	0.01	0.01	0.01	0.01
scenario 2	0.6	1.2	0.01	0.005	0.004	0.004	0.004	0.004	0.004	0.004
time	0.9 s	2.3 s	13 s	28 s	33 s	73 s	77 s	75 s	132 s	229 s

Table 3: Error comparison for the two scenarios together with time used for test network 1

pressure plot in Fig. 2.

Firstly, only a part of this function is used as training data, i. e. every k-th time step, $k = 9$, of a simulation ($\Delta t = 100\,\text{ms}$) is used to set up our POD projection matrix, just as in the simplest case described in Sect. 5. We then use all available 100 time steps in order to compare the solution obtained by POD reduction to the original solution. Secondly, we use all available time steps as training data to set up our second POD projection matrix, not only every k-th time step. We then compare the solution of the reduced system and the full system for a slight variation of the input function given by

$$s(t) = (1 - 0.085(\cos(t\pi/1000) - 1))\, S_0.$$

The latter test case is relevant from a practical point of view because it resembles the situation, where a series of parametrized solutions has to be computed in order to either analyse the system or find a starting solution for a periodically re-measured input.

The pressures and fluxes at the supply node as well as at node 9 are plotted in Figs. 2–13, where Figs. 2–7 refer to the first scenario, while Figs. 8–13 illustrate the second one. Here, the flux plots of a node refer to the sum of the q_L^k of all pipes k entering at that node. We solve the system as given in [GHK$^+$13, Eqns. (6)–(10)] with the function `fsolve` from [JOP$^+$]. The implementation is not optimized, but should allow for comparing the run time of the original solution to that of the reduced system. The average running time of 100 executions (including computation of input, system solution, storage routines) of the original system of size 65 (notice the additional equations in [GHK$^+$13, Eqns. (6)–(10)]) has been measured as 2.28958848953 s. Making use of some sparse matrix routines, we can decrease this run time to 0.685134909153 s for the POD reduced system. The measurement now also includes the expansion of the reduced state.

As emphasized before, the results we mainly report here refer to a very simplified problem. Still, this index 1 problem is already challenging to simulate in its original DAE form. Reducing it via POD often makes the solution numerically more unstable and thus more difficult to solve. A greater difference between the input used to set up the POD and the input used to test the reduction can already lead to numerical problems within this setting. The reported errors are acceptable, but might add up to unacceptable errors in larger networks.

Simulating that same problem within the ODE framework described in Sect. 4 is comparatively simple and straightforward (Matlab's ODE solver can be used directly to achieve accurate and fast results). Even strongly reducing it to an order size of 4 results in but a small error, which indicates that this method is more suitable for larger networks than the direct approach.

Table 3 shows the errors for the two scenarios and different reduction orders.

We can see that the time grows over the time of simulating the full order system for $r = 12$. This is not surprising since we do not apply any technique to deal with the nonlinearity in an efficient way. We can furthermore see that the error stagnates. We are computing an

absolute maximum error over all variables. If we look, however, at the maximum error of the pressure curve at node 9 for example as we did above we only have an absolute max error of 10^{-6}. We did not further investigate the origin of that stagnation since the reduced order model of size 8 gives good overall results. More tests have been conducted with the following supply function

$$s(t) = (1 - 0.2(\cos(t\pi/1000) - 1))\, S_0.$$

The maximum error for the reduced order of size 8 was 0.02 in that case.

The second example, which is a realistic part of a gas network, is a little more challenging and due to the fact that it has more than one supply it no longer has index 1. The topology of the graph is shown in Fig. 14. This system has 45 nodes and 47 pipes. Which leads to an ODE system of size 88 since we have 4 supply nodes. Simulating this network in the DAE form can already be slightly challenging. Reducing it in the naive way typically does not lead to a numerically stable system anymore in practice. Model Order Reduction techniques for nonlinear differential algebraic systems are not very well understood and even in the case of linear problems one typically has to address the subject and take apart the differential and algebraic contributions [BS13].

This network has been simulated with a demand function $d(t) = d_0 \times t/3600$ in the first hour and then constant. The network has two demands, which are set to $0.4\,\mathrm{kg/s}$ and $0.3\,\mathrm{kg/s}$. In the first hour of operation we linearly increase them and then keep them constant. The supply is slowly lowered at one supply node in a C^1 fashion over 3 hours. We then reduce the system to size 8 and simulate again. The maximum absolute error is then 0.1. However the mean absolute error is 0.01. These results seem very promising and future work should include larger networks as well.

7 Discussion

In our work described here, we study the numerical simulation of gas transport within pipeline networks that consist of pipes only. More involved components have not been considered. Given a simplified differential system to capture the physics of gas transport, mass balance laws for the network, as well as a discretization in space, we derive a nonlinear DAE. We furthermore show that the problem lies in a class of DAEs that have Tractability Index 2 or lower, relate the index to the network topology, and give an alternative formulation with better tractability, namely an Ordinary Differential Equation. We discuss the application of Model Order Reduction by Proper Orthogonal Decomposition to both the original system and the index-reduced ODE.

We also present numerical results for two examples, a smaller index 1 network and a somewhat larger index 2 network. The small network is tested in two settings. In the first setting we use few snapshots of a time series with varying supply pressure in order to construct an order-reduced system by POD and compare the solution of this reduction to the original system. In a second setting we use all available time steps for the construction of our POD projection. We then test the reduced system with respect to a slight variation of the input functions and obtain a reduction error that is acceptable but higher than in the first setting. The larger network is tested within some basic test case, that shows promising future applications.

These numerical tests give first evidence that the numerical solution and Model Order Reduction of the equivalent ODE formulation is more stably achieved yielding more accu-

rate solutions than that of the original system. Notice that we have splitted MOR into two independent projections for the ODE which can also explain the better results.

The simplifications we suppose are motivated by industrial practice as well as by certain specific problems that can arise in scenario analysis (analysis of input or parameter variations) or in finding a starting solution for a complex network via the solution of simplified but increasingly more complex sub-problems. Nevertheless, further components ought to be considered in future research in order to allow for the Model Order Reduction of a larger class of pipeline networks from the engineering practice. The tractability of MOR systems of DAEs should perhaps be discussed and investigated more deeply in order to gain a better understanding of the matter if a system cannot be transformed as straightforwardly into an ODE as we have seen here. Such a discussion should comprise a more detailed analysis and numerical examination of our concluding remark in Sect. 5.2. In future work, the topological meaning of the presented results could be considered. Also, (16) might represent an ideal starting point to discuss the effects of topology *changes* on the original system as well as on MOR approaches.

References

[BS13] Nicodemus Banagaaya and Wil Schilders. Simulation of electromagnetic descriptor models using projectors. *Journal of Mathematics in Industry*, 2013.

[ES] Klaus Ehrhardt and Marc C. Steinbach. Nonlinear optimization in gas networks.

[GHK+13] Sara Grundel, Nils Hornung, Bernhard Klaassen, Peter Benner, and Tanja Clees. Computing surrogates for gas network simulation using model order reduction. In Slawomir Koziel and Leifur Leifsson, editors, *Surrogate-Based Modeling and Optimization*, pages 189–212. Springer New York, 2013.

[HK12] Michael Hinze and Martin Kunkel. Discrete empirical interpolation in POD model order reduction of drift-diffusion equations in electrical networks. Berlin: Springer, 2012.

[HMS10] M. Herty, J. Mohring, and V. Sachers. A new model for gas flow in pipe networks. *Mathematical Methods in the Applied Sciences*, 33(7):845–855, 2010.

[Jan13] Lennart Jansen. A Mixed Index Concept: The Tractability-Strangeness Index. *DAE Forum*, 1, 2013.

[JOP+] Eric Jones, Travis Oliphant, Pearu Peterson, et al. SciPy: Open source scientific tools for Python, 2001–.

[JP13] Lennart Jansen and Jonas Pade. Global Unique Solvability for a Quasi-StationaryWater Network Model. *DAE Forum*, 1, 2013.

[KV02] K. Kunisch and S. Volkwein. Galerkin proper orthogonal decomposition methods for a general equation in fluid dynamics. *SIAM J. Numer. Anal.*, 40(2):492–515, 2002.

[LIW04] LIWACOM Informationstechnik GmbH, Simone research group, Essen. *Simone Software: Gleichungen und Methoden*, 2004.

[LMT13] R. Lamour, R. März, and C. Tischendorf. *Differential Algebraic Equations: A Projector Based Analysis*. Springer, 2013.

[Meh13] V. Mehrmann. Index concepts for differential-algebraic equations. *Preprint*, 2013.

[RR11] W. Marquardt R.C. Romijn, S. Weiland. Proper orthogonal decomposition for model reduction of linear differential-algebraic equation systems. In *Proc. 18th IFAC World Congress, Milano*, 2011.

[Sir87] L. Sirovich. Turbulence and the dynamics of coherent structures. parts I-III. *Quart. Appl. Math.*, 45(3):561–590, 1987.

[Ste07] Marc C. Steinbach. On PDE solution in transient optimization of gas networks. *Journal of Computational and Applied Mathematics*, 203(2):345–361, June 2007.

[Tis99] C. Tischendorf. Topological index calculation of DAEs in circuit simulation. *Surveys on Mathematics for Industry*, 8(3-4):187–199, 1999.

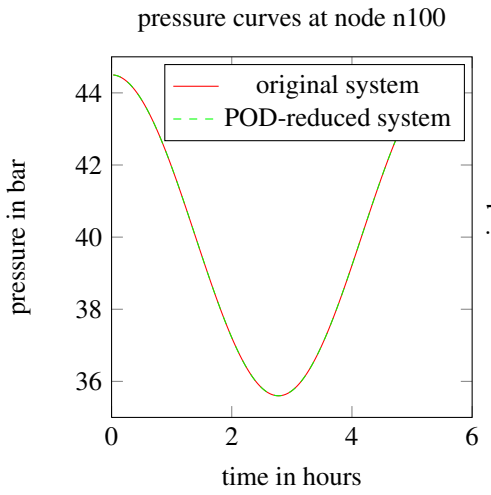

Figure 2: Pressure at the supply (given)

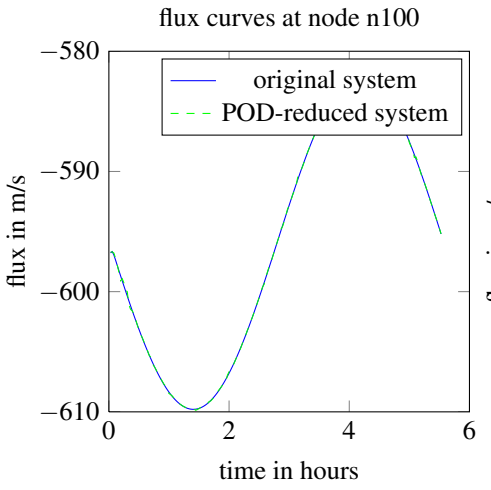

Figure 3: Flux at the supply

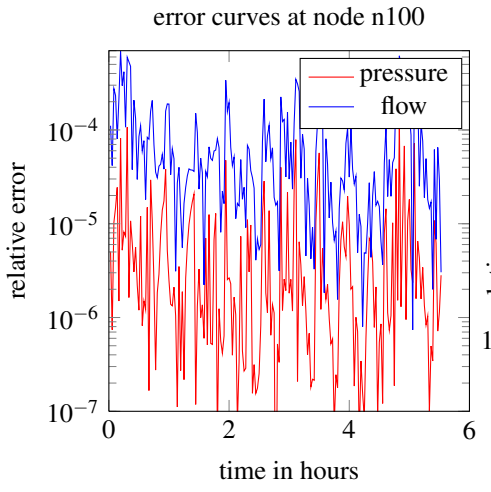

Figure 4: Pressure and flux error at the supply

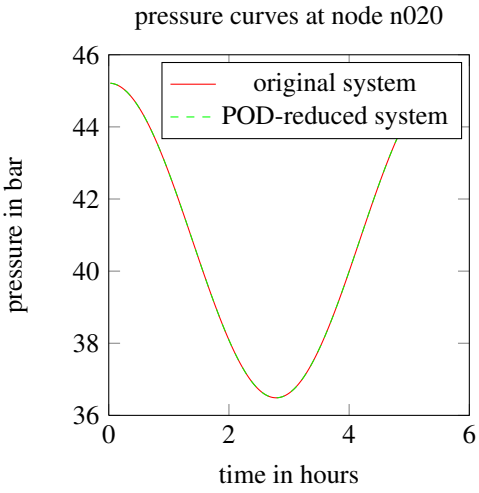

Figure 5: Pressure at node 9

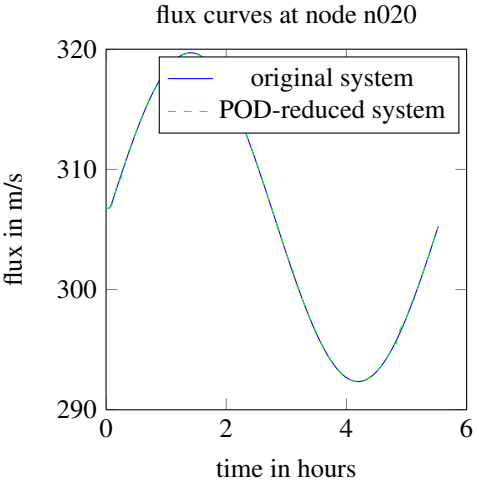

Figure 6: Flux at node 9

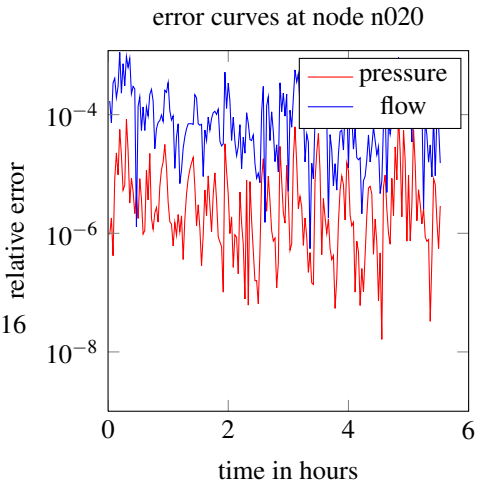

Figure 7: Pressure and flux error at node 9

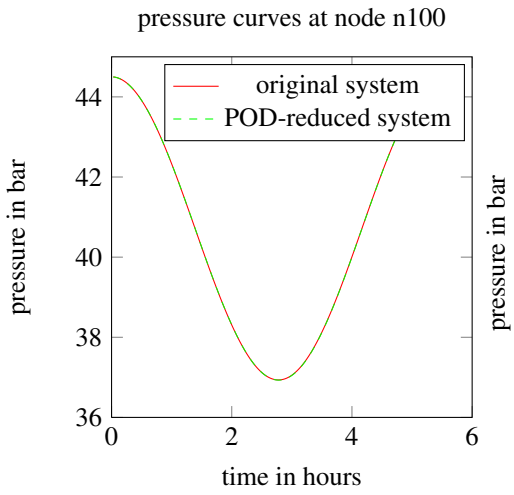

Figure 8: Pressure at the supply

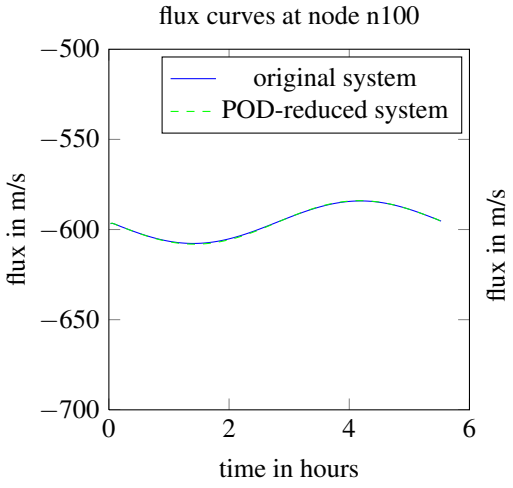

Figure 9: Flux at the supply

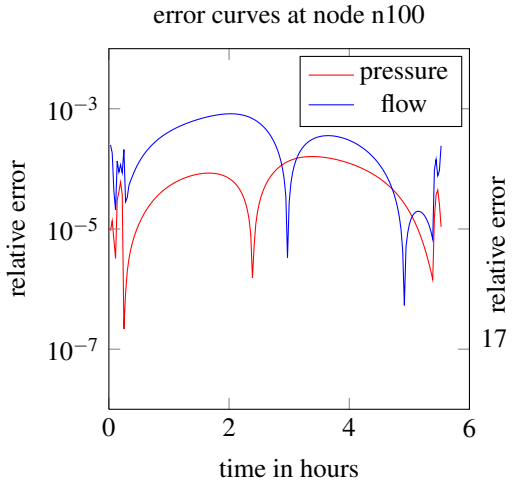

Figure 10: Pressure and flux error at the supply

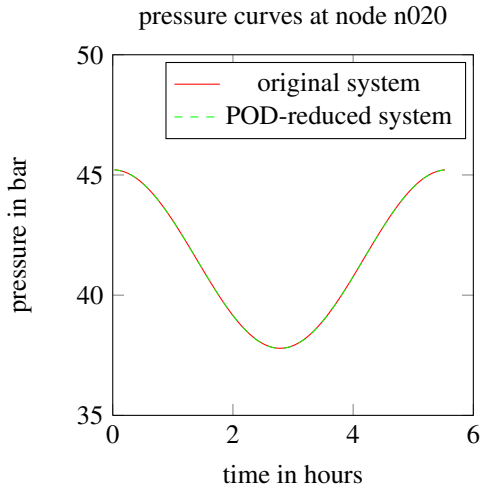

Figure 11: Pressure at node 9

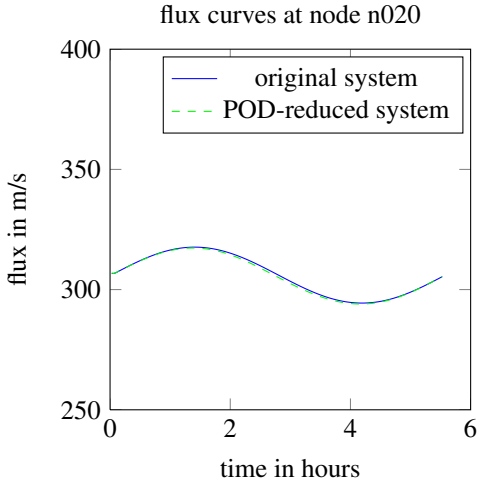

Figure 12: Flux at node 9

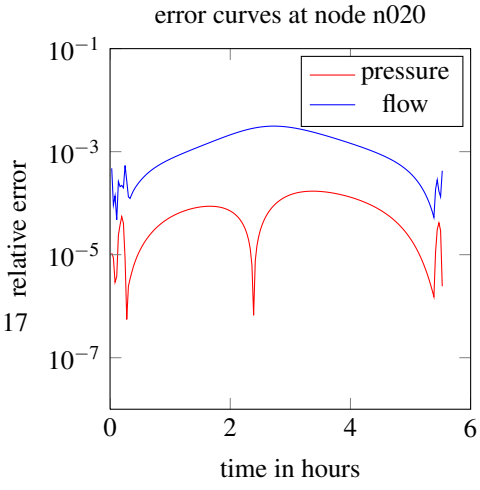

Figure 13: Pressure and flux error at node 9

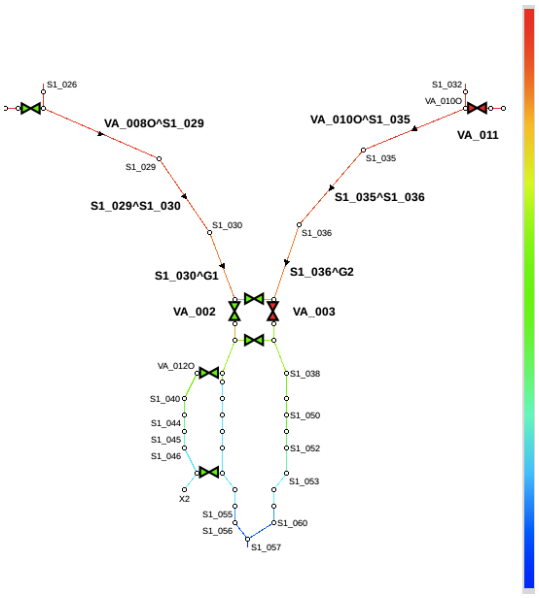

Figure 14: Gas network graph 2

Max Planck Institute Magdeburg Preprints